How can mining data be used for regional stress derivation ? – Recommendations Based on Examples from the Ruhr Area

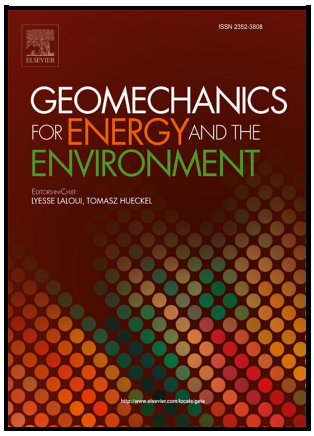

Thomas Niederhuber, Martina Rische, Birgit Müller, Thomas Röckel, Felix Allgaier, Kasper D. Fischer, Frank Schilling, Wolfgang Friederich

PII: S2352-3808(25)00013-9

DOI: https://doi.org/10.1016/j.gete.2025.100648

Reference: GETE100648

To appear in: *Geomechanics for Energy and the Environment*

Received date: 21 August 2024
Revised date: 16 January 2025
Accepted date: 5 February 2025

Please cite this article as: Thomas Niederhuber, Martina Rische, Birgit Müller, Thomas Röckel, Felix Allgaier, Kasper D. Fischer, Frank Schilling and Wolfgang Friederich, How can mining data be used for regional stress derivation ? – Recommendations Based on Examples from the Ruhr Area, *Geomechanics for Energy and the Environment,* (2025) doi:https://doi.org/10.1016/j.gete.2025.100648

How can mining data be used for regional stress derivation ? – Recommendations Based on Examples from the Ruhr Area

Thomas Niederhuber[1], Martina Rische[2], Birgit Müller[1], Thomas Röckel[3], Felix Allgaier[4], Kasper D. Fischer[2], Frank Schilling[1], Wolfgang Friederich[2]

[1] Institute of Applied Geosciences, Karlsruhe Institute of Technology, Division of Technical Petrophysics, Karlsruhe, Germany (thomas.niederhuber@kit.edu)
[2] Institute of Geology, Mineralogy and Geophysics, Ruhr-University, Bochum, Germany
[3] Piewak & Partner GmbH, Bayreuth, Germany
[4] Institute of Applied Geosciences, Karlsruhe Institute of Technology, Division of Structural Geology, Karlsruhe, Germany

Corresponding author: Thomas Niederhuber (thomas.niederhuber@kit.edu); Institute of Applied Geosciences, Karlsruhe Institute of Technology, Division of Technical Petrophysics; Adenauerring 20b, Karlsruhe, Germany; Tel.: +49 721 608-45221

Keywords:

- Stress State in mines
- Stress Concentrations
- Eastern Ruhr Mining Area
- Pore Pressure Around Mines
- Hydraulic Fracturing Tests

Abstract

Due to the wide availability of stress measurements in mines it is tempting to infer the regional stress state from stress observations in mines. However, our study demonstrates limitations of this approach and how to overcome them. In this study we used hydraulic fracturing measurement data from shallow boreholes at different mining depth levels in the eastern Ruhr area and compared them with stress information from deep boreholes to infer the regional stress state. We defined selection criteria , which resulted in more robust values for S_{hmin} magnitudes because we eliminated the data that had been influenced by the mine galleries, mining sequence and nearby faults. When deriving S_{Hmax}, special consideration was given to the effect of pore pressure. Despite the fact that mines are filled with air, pore pressure cannot be automatically assumed to be zero. The pore pressure in the tested intervals is highly dependent on the excavation damage zone and the permeability of the rock. We show that careful selection of data and consideration of pore pressure (for S_{Hmax} values) is essential to distinguish between local and regional stresses in mining areas. We therefore recommend the use of independent pore pressure observations and, where available, deep vertical borehole data. The resulting stress state in our study is indicative of normal fault tectonics, contradicting previous studies that infer a strike-slip tectonic regime. This results in less critical stress states of faults in the study area.

Plain Language Summary

Using stress measurements from mines to understand regional stress has limitations. We studied hydraulic fracturing data from short boreholes in mines and deep boreholes in the north-eastern Ruhr area. We carefully checked each measurement and set criteria like distance to tunnels, proximity to faults, and sequence of mining, which result in more accurate S_{hmin} values by excluding affected data. For S_{Hmax} calculations, we considered pore pressure. Even though mines are filled with air, pore pressure isn't necessarily zero. It depends on the damage zone around the excavation and the rock's permeability. To distinguish between local and regional stresses, we suggest to choose data carefully and consider pore pressure for S_{Hmax} determination. Where possible additional data from deep boreholes should be used. Our study shows that the stress state is a normal faulting tectonic regime.

1 Introduction

Understanding the stress field in mines is crucial for ensuring safe and efficient underground operations. Different methods have been developed to assess stress conditions for engineering purposes. Early investigations of the magnitude of stress in mines, pioneered by Hast [1], were based on overcoring observations. His work included more than 15,000 discrete stress measurements across 30 sites in Scandinavia. In recent decades, hydraulic fracturing (HF) tests, which were introduced in the 1960s [2] have progressively replaced overcoring. In the Ruhr mining district substantial measurements have been conducted by researchers such as [3-5] and MeSy (now MeSy Solexperts). Further technologies are used (e.g. [6-8]) to derive the local or regional tectonic stress field with its principal stress components (S_{Hmax}, S_{hmin} as maximum and minimum horizontal stresses and S_V as vertical stress). The World Stress Map (WSM) sets

standards for the quality of stress observations, focusing primarily on the regional state of stress [9,10].

The stress field, along with rock properties, is critical for assessing mine safety, particularly regarding rock failure. Mining-induced seismicity and rock bursts often correlate with changes in stress conditions, posing significant safety risks to personnel and infrastructure. In the German coal mining in the Saarland region [11], the occurrence of induced seismicity has led to the cessation of mining operations. Rock bursts, characterized by instantaneous failures in areas of increased stresses in underground openings are common in mine workings, pillars, tunnels, and shafts with substantial overburden [12] and contribute significantly to the overall seismicity.

Stress observations in mines cannot directly infer the regional stress state due to the combination of regional stress and local stress concentrations. In the vicinity of mines, shafts, tunnels, caverns and other underground openings, the zero shear stress boundary conditions cause reorientation and stress concentration (stress arching, [13-16]) in the remaining structures. Thus, close to free surfaces (quarry walls, tunnels, mines) the stresses do not necessarily reflect the regional stress state. Therefore, even if a stress observation near the excavation itself provides perfect data quality according to WSM, it is only representative of the near-field stress and not necessarily to the regional stress state.

Accordingly, criteria for evaluating different types of stress information have been established for the purpose for regional stress analyses. Zoback [6] proposed the utilisation of a quality ranking table for stress indicators, with the objective of assessing the reliability of data for regional stress orientation. The modern WSM quality ranking table employs a grading system from A to E [17], with A-C grades indicating reliable regional horizontal stress orientation indicators.

As HF and overcoring observations in mine galleries and shafts are significant for mining operation safety, numerous measurements exist worldwide [19,20] and allows for the derivation of the regional state of stress. It is tentative to interpret the vast amount of this data to get a more detailed database for numerical modelling or to infer the reactivation of faults. The different quality of the data needs to be considered, as stress relief data obtained by overcoring with a small distance to a free surface (less than 10 m) are classified with a quality designation of E [10]. Higher quality levels require measurements at depths greater than 10 m from the nearest free surface, with quality B requiring a minimum distance from the excavation equal to at least two excavation diameters (WSM) [18]

For hydraulic fracturing data, the WSM quality assessment is based on hydraulic fracturing measurements obtained from boreholes drilled from the ground surface. Boreholes within mining operations are typically shallow and show the same limitation than overcoring data. Hence the damage zone needs to be taken into account and the same criteria as for overcoring data should apply for HF data within mines. Morawietz [9] used the WSM quality ranking to introduce a stress magnitude classification scheme, though classification for HF measurements from shallow underground boreholes is still missing.

One of the most comprehensive compilations of mine HF data for the study area (Ruhr area) is presented in [21], with the averaged results of 423 HF measurements taken at six mines between 1986 and 1995. These are classical HF tests with straddle packers and all measurements that were quality-weighted according to the criteria outlined by WSM [9]. However, the

representativeness for the regional stress field was not evaluated. The tectonic stress field in the eastern Ruhr area is characterized by a NW-SE oriented compressive stress, which is accommodated by a series of thrust faults and folds in the sedimentary rocks of the region. However, the stress field is also influenced by local structures, such as the normal faults, which form Horst and Graben structures. Niederhuber [22] compile stress orientations and show how data from shallow boreholes inside mines can be used to derive stress orientation [22]. Combined with other data sets like the World Stress Map database [8], gridded stress orientation maps have been created[22].

One limitation of the HF method is that it provides a direct measurement of the minimum stress magnitude only. In order to derive the maximum horizontal stress magnitude from the measurement of the minimum stress magnitude, it is necessary to know the pore pressure. In many cases, however, the pore pressure is unknown. In permeable or highly fractured rock, the pore pressure in the vicinity of an opening is close to zero. Conversely, in dense and tight rock, the pore pressure may remain elevated and largely unaffected by the opening. Incorrect assumptions about pore pressure can result in the derivation of erroneous maximum horizontal stress magnitudes and an inaccurate characterization of the tectonic regime.

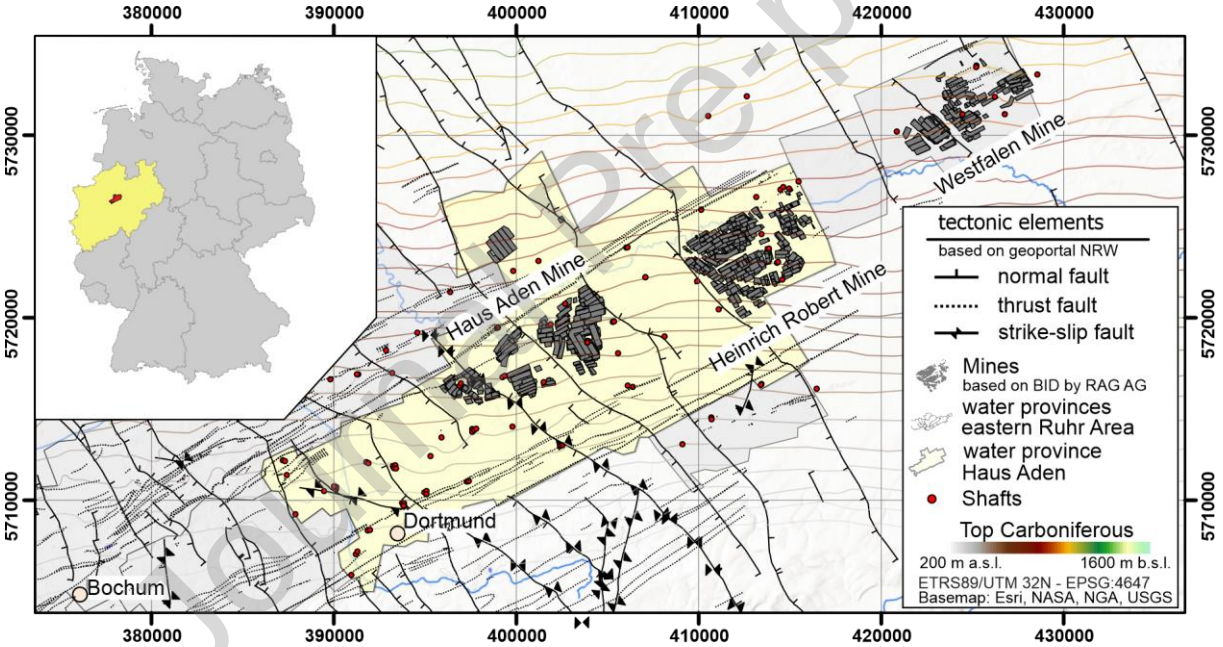

Fig. 1: Map of Study Area in the eastern Ruhr Area including the water provinces (central pumping stations for water regulation in mines; location of shafts; locations of the mines Haus Aden, Heinrich Robert and Westfalen; tectonic elements and top Carboniferous based on Geologischer Dienst NRW [23].

This study aims to determine the regional stress state and the pore pressure conditions for the Ruhr area at water province Haus Aden, which is of particular importance due to current mine-flooding activities (Fig. 1). The database includes information from deep boreholes and stress observations in mines. To achieve this goal, we re-evaluate the HF-measurement data from deep boreholes in the Ruhr area, taking into account the influence of the measured pore pressure. We use the density logs of these wells to derive the vertical stress component. To determine the regional stress from the mine measurements in the study area, we applied selection criteria to separate those measurements that indicate local stresses from those that provide regional stress

information. From our results we provide recommendations for the use of HF stress magnitude data to derive the regional stress state that could potentially be included into the WSM quality ranking.

2 State of the Art: Factors Influencing the Stress Field in Mines

Here we briefly summarize natural (lithology and distance to faults) and anthropogenic factors that need to be considered for the local state of stress in mines.

2.1 Modifications due to Lithology and Faults

Variations in lithological units or the degree of rock fracturing often result in changes in the rheological properties and material parameters of the rock, which can affect the stress magnitude and orientation [7,24]. These changes have been measured by different methods like HF measurements and strain recovery [25]. In their experiments in oil and gas fields the S_{hmin} magnitudes in shales in the North Sea were significantly higher than the magnitudes measured in sandstones [26]. Similar observations are shown by e.g. [27]. In a compressional stress state the stress magnitudes of the least principal stress correlate with the stiffness of the rocks [28]. More recently these effects have been proven by numerical studies (e.g.[29,30]).

Furthermore, geological structures like faults, fractures, folds, and other structural features can concentrate or dissipate stress and can therefore lead to changes in stress magnitude and orientation. In folds the stress state can be extremely heterogeneous ranging from extensional to compressional nearby areas as a result of the shape of the fold [31]. For frictionless discontinuities such as faults and joints, stress rotations have been observed from borehole to regional scale [32-36]. The rotation is facilitated when the differences in principal stress magnitudes are small [17,37,38].

2.2 Changes due to Mine Geometry and Mining

Anthropogenic activities in the subsurface can modify the local state of stress and also the pore pressure. For example, each opening of the subsurface such as mines, boreholes or tunnels leads to new surfaces with zero shear stress and thus modifies the stress magnitude and usually rotates the principal stresses [39,40]

Unloading and new free surfaces lead to stress concentrations [41] around the underground opening which had been focus of numerous analytical and numerical studies. In the zones of stress concentrations, rock failure lead to a) rock fracturing due to excessive compressive or tensile stresses, b) opening or closing of pre-existing fracture or shearing along them and thus form excavation damage zones with stress relief and changes in hydraulic conductivity [42]. In the excavation damage zone, the material stiffness is reduced. Triaxial tests show that these damage zones affect stress measurements [43] up to a distance of three times the tunnel diameter (six times the radius) [4].

Removal of large masses of material in the subsurface can modify the vertical load in some sections and due to stress arching effects, lead to vertical stress increase in other parts, such as the remaining pillars in within the mined out areas [44]. At the bottom of the mined out areas tensile stresses can develop [45]. However, also changes in deviatoric stress components e.g. in South Africa can explain mine tremors [46].

Stress concentration and stress arching effects may superimpose. In general, the zone around a mine opening can be characterized by the so-called excavation damage zone where the rock is fractured (and thus destressed) and at some distance from the opening, the undisturbed zone where the regional stress field is encountered (Fig. 2). In between there is a transition zone which may still exhibit compressive or tensile tangential stress concentrations, depending on the tectonic regime, the orientation of the mine and the amount of mined out material, respectively.

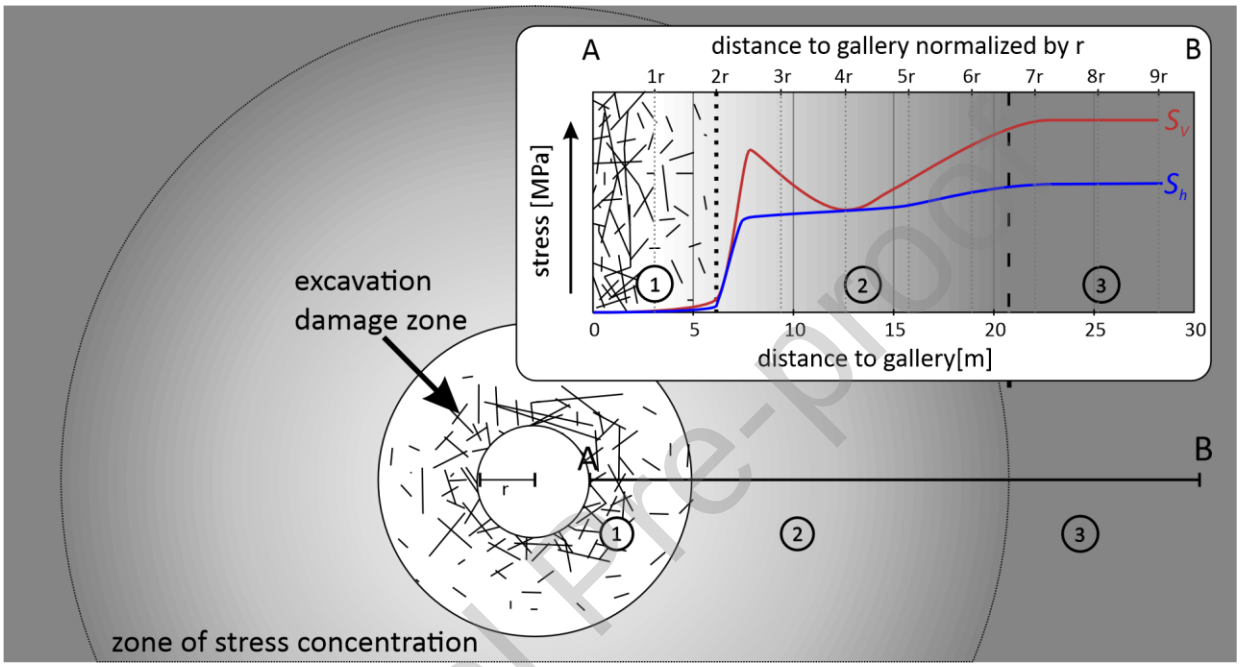

Fig. 2: Schematic representation of the damage zone and the zone of stress concentrations around a cavity. (1) almost complete release of stress; (2) zone of stress concentrations; (3) rock subjected to far field stresses without stress concentrations (figure according to description of [4,43])

Undercut-mining can lead to severe, in stress mapping literature sometimes not considered, changes of the stresses in the undercut mine level [47-49]. If a mine has been caved and mined out, high stress levels develop around the perimeter of the mine which affect stability. A second level below the caved extraction destresses the rock and enables further mining. The upper level becomes then an undercut level. The upper undercut level should be completed first enabling that the lower tunnels are carried out in a destressed rock [49]. There are different methods of undercutting depending on the sequence of development mine-levels: a) In post-undercutting or conventional undercutting the deeper production level has been completed first and then, the shallower undercut level is developed. 2) In pre-undercutting the undercut level is completed before the development of a production level in deeper sections. 3) In advance undercutting the excavation takes place above a deeper partially developed production level.

As the objective of undercutting is to destress the mine in the production level, the stress magnitudes are decreased in comparison to the far field stresses. Thus, to infer the regional stress field, the sequence of mining and hydraulic fracturing in the mines are considered here.

3 Geological Setting and Mine Description

3.1 Geological and Tectonic Setting

The Ruhr Basin is an Upper Carboniferous (Pennsylvanian) sedimentary basin in western Germany. The basin extends approximately 150 km in NE-SW direction and about 80 km across [50,51] and is home to the largest domestic coal mining area in Germany. In 2018 mining operations were ceased[52].
In a warm and humid climate during the Westfalian period, extensive forest (peats) bogs and bog (peat) lakes were formed in a shallow, constantly sinking coastal area. When the sedimentation rate was slower than the subsidence, sea flooding occurred resulting in the deposition of sea sediments. The interplay between the renewed filling of mud and sand masses, increasing sedimentation and peat formation took place in approximately 350 cycles. As the sediments and peat deposits sank to greater depths, claystone, siltstone, sandstone and hard coal were formed. The coal seams represent approximately 2-3 % of the total layer sequence [53].
The thicknesses of the stratigraphic sequences and of the coal seams were obtained from deep drillholes and from the mines. The Carboniferous strata terminate at the surface in the southern part of the Ruhr area. In the northern region, these geological formations are situated at considerable depths beneath the Cretaceous strata [54]. In the study area the base of the Cretaceous is situated at a depth of between 250 and 750 m below sea level (see Fig. 1).
The thickness of the Upper Carboniferous was determined in the Münsterland 1 borehole, situated to the north of the study area. The Top of the Upper Carboniferous was observed at a depth of 1788 m [55,56], marking the boundary with the Carbonaceous rocks and extending to a depth of approximately 5438 m. The boundary between the Lower Carboniferous and Devonian is at a depth of 5507 m [56]. This corresponds to an apparent thickness of the Carboniferous of 3719 m. The dip of the strata in the borehole Münsterland 1 is predominantly between 2° and 18°. Occasionally a dip angle of up to 85° is also described [56]. However, this is only likely to be the case in fault zones. Therefore, the true thickness of the Carboniferous is likely to be around 3500 m [57] with approximately 100 coal seams [58].

The Ruhr Basin is characterized by thrust faults and dominant NW-vergent folds of Variscan origin [59], subdividing the area into NE-SW trending anti- and synclines [50]. Normal faults striking NW-SE to NNW-SE separate the area into Horsts and Grabens. In addition, E-W and N-S trending strike-slip faults are present [50]. The mining areas of this study are located within the Essen syncline (Essener Mulde) and the Bochum main syncline (Bochumer Hauptmulde). Both are bordered to the WNW and ESE by the Sutan and Scharnhorst thrust faults respectively. The Sutan fault is considered as the major tectonic structure extending laterally for more than 100 km [52]. Furthermore, the Königsborn fault, the Flierich fault, and the Radbod fault (a normal fault) subdivide the area into the Königsborn Graben and the Hamm Horst (Fig. S.1).

The coal mining followed these structures. Due to the alternating layers along with the Horst and Graben structure, the mining levels in each mine are at different depths. The average economic relevant coal seam thickness ranges between 1-3 meters [60]. Many strike slip (transverse and diagonal) faults in the basement were formed post-Variscan and during the Alpine orogeny [61-63]. Presently, these faults and the Ruhr area exhibit very low natural seismic activity, as confirmed by the 2011 seismic zoning map (DIN EN 1996), which places the Ruhr area outside seismic zoning ranges [64]. This low seismicity is supported by studies indicating a

generally low slip tendency of the faults e.g. [65] who did calculations for the faults around Heinrich Robert mine or [66] who used a statistical approach and lithology dependent friction coefficients taking into account the heterogeneities of the layered rocks.

3.2 Haus Aden Mine

Haus Aden which is part of the "Bergwerk Ost" colliery in the Eastern Ruhr region, consists of the formerly independent mines Haus Aden, Monopol and Heinrich Robert [67]. The mine development was a step-by-step process, with different mining levels established at different times. Essential for maintaining safe mining conditions was an effective mine water drainage. Since coal mining has ceased, long-term optimization of drainage remains a perpetual obligation. The RAG plans to centralize mine water management at several key sites in the Ruhr region, with Haus Aden designated as one of these "water provinces."

Coal production in the Haus Aden started in 1943 using longwall mining techniques, partly with hydraulic roof supports protecting the area. Similar to other German hard coal deposits, productive seam thickness varies between 1-3 meters [60], with an average seam thickness at Haus Aden of about 2 meters (Fig. S.2.1; Fig. S.2.2). Between mined sections pillars are left in place. Some sections of the excavated areas are refilled by waste.

The design of the mine is described in supplement 2. The mining area of Haus Aden was developed following the structure of the coal seams located in Carboniferous rocks within NE-SW striking folds (Fig. S.2.3). The mining activity has encountered initial and thus undisturbed stress conditions, while in other places already mined zones have encountered modified stress conditions by nearby galleries. This also affects the determinations of tectonic stress in the Ruhr area (see [22] and section 3). Undercut mining has been performed in different sections of the mine [68]. Here, we consider especially the area around shaft 6 where HF-measurements have been performed at a depth of 750 m before and after post-undercut mining at a level of 880 m depth.

4. Results from borehole data analysis

4.1 Pore pressure compilation

Pore pressure is an important parameter in the evaluation of flood-induced stress changes and required for the calculation of S_{Hmax}. In hydraulically connected formations which are not disturbed by injection, pumping, or groundwater lowering, pore pressure can be determined by integrating fluid densities (ρ_f) over depth (z) starting from a pressure head (z_{ref}).

$$P_P = \int_{Zref}^{z} \rho_f(z) g \, dz$$

In this study we investigate the pressure distribution on a regional scale and in the mining areas. The regional pore pressure gradient was determined from mineralization of water samples in reports from [69] and [70] described in supplement 3 and from data of the Münsterland-1, Rieth-1 and Natarp-1 wells (supplement 4). In the Münsterland-1 well the pore pressure information comes from drill stem tests [71]. In Rieth-1 and Natarp-1(Fig. 3a) packer tests [72] were re-evaluated in the framework of this study to derive the pore pressure. The mineralization indicates a range of pore pressure gradients between 10.3 and 10.4 MPa/km (supplement 3). The pore pressure gradients from boreholes are 11.6 MPa/km (Münsterland-1), 10.4 MPa/km (well Rieth-1) and 10.6 MPa/km (well Natarp-1) at greater depth.

4.2 Vertical stress

Litho-density logs from 14 deep boreholes provided by the Geologischer Dienst NRW (geological survey of North Rhine Westphalia) and densities from core investigations [73-75] were used to estimate vertical stress as lithostatic load (Fig. 3a, supplement 6). The average density of the Upper Cretaceous, based on litho-density logs is 2380 kg/m³. For the Carboniferous, the average density is 2540 kg/m³ (based on litho-density logs) and 2610 kg/m³ (based on core data), resulting in an average density of 2570 kg/m³. For details we refer to supplement 6.

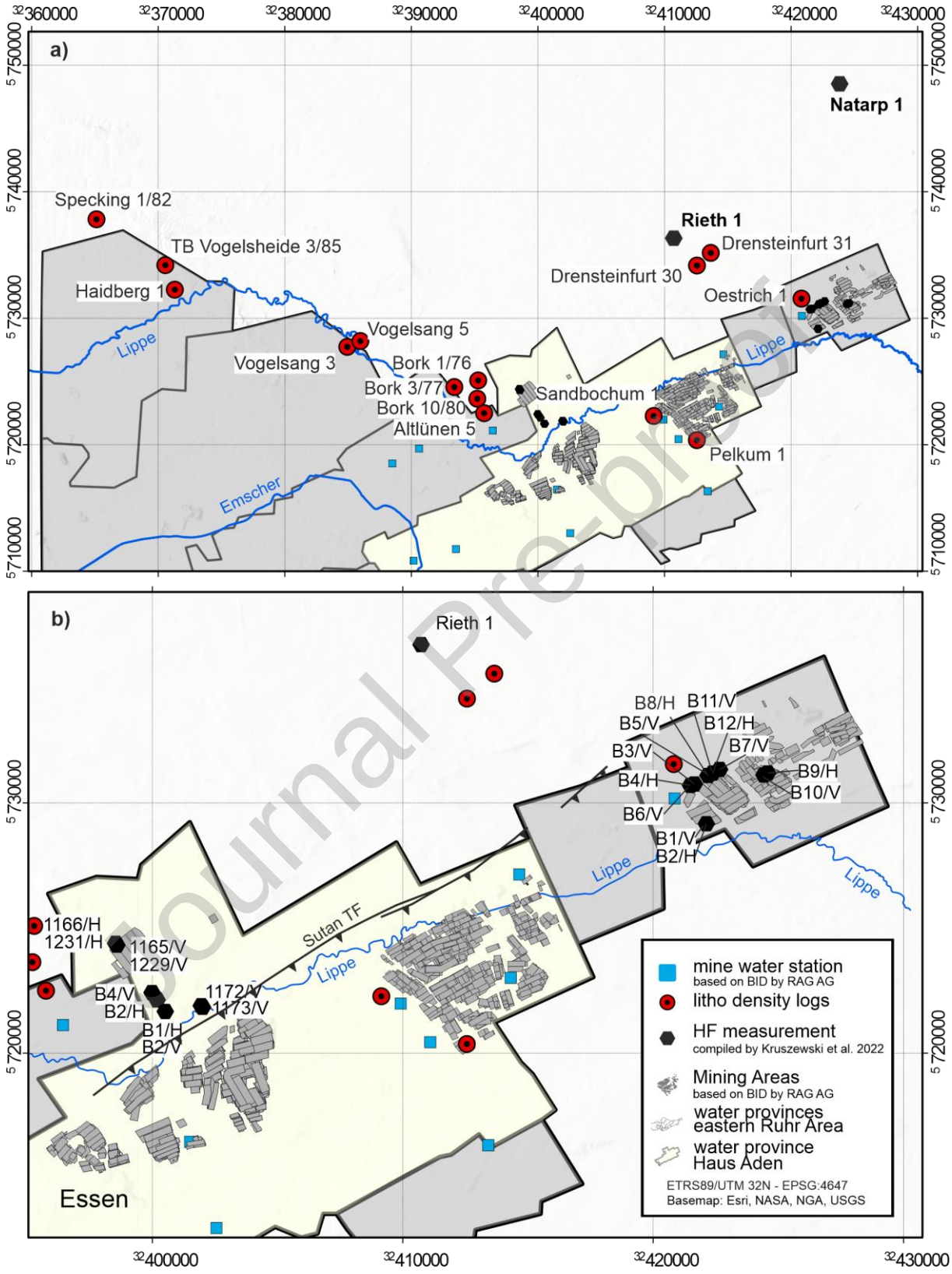

Fig. 3: a) Overview maps with location of the analyzed boreholes of the litho-density logs, the location of the HF measurements based on [21]; b) Detail of the three mines Haus Aden, Heinrich Robert and Westfalen with the trace of the Sutan TF based on [66].

4.3 Stress Magnitudes with Depth

The hydraulic fracture test results from both boreholes (Rieth-1 and Natarp-1) are in accordance with a linear increase with increasing depth. The S_{hmin} gradient derived from HF measurements in deep boreholes Rieth-1 and Natarp-1 (Fig. 9) is 15.6 MPa/km±0.8 MPa/km. The S_{Hmax} gradient in Rieth-1 and Natarp-1 derived in this study by applying the measured pore pressures within the boreholes Rieth-1 and Natarp-1, respectively, is 20.4±2.3 MPa/km (the details of the analysis can be found in supplement 7). The vertical stress has been calculated using an average vertical stress gradient of 24.4 MPa/km.

5. Selection of *in-situ* Stress Observations in Mines to Derive the Regional Stress Magnitudes

The tectonic stress field in the eastern Ruhr area has been the subject of numerous studies [3-5,21,76,77] which are based on HF-measurements and borehole data. The recent compilation by Kruszewski [21] with 429 data entries [78] shows high variability in the stress gradients of S_{Hmax}, S_{hmin} and S_V magnitudes and, in most cases, the information about the deduction of stress magnitudes is not complete, which complicates the derivation of the regional patterns of tectonic stresses. This especially concerns the pore pressure at individual locations. To reduce the uncertainty in stress magnitudes the data was analyzed for different potential influencing factors, including the effect of tested lithologies, the sequence of mining, and distance to nearby galleries.

5.1 Influence of Lithology

To study the potential influence of the lithology we sorted S_{hmin} data given in [79] according to the rock types (Fig. 4). There is no general trend for the S_{hmin} gradient observed across the sandstones, sandstone-claystone alternations, and claystone lithologies. Most groups have high uncertainties (indicated by the size of the boxes and length of the error bars in the box plot). However, there is some evidence that the S_{hmin} magnitude is underestimated in heavily jointed rocks. Therefore, tests in highly fractured boreholes like B4/H, B7/V and B9/H in the Westfalen mine have been excluded from our analysis of the regional stress field.

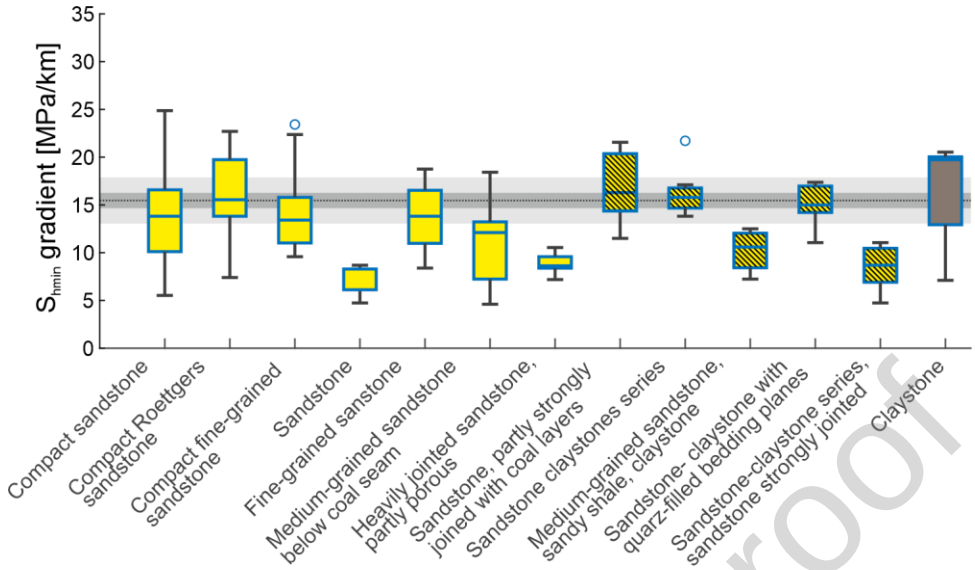

Fig. 4: Visualization of the S_{hmin} gradients based on the lithology in which the test was conducted (sandstone: yellow, sand-claystone alternation: yellow with brown hatching, claystone: brown). The dashed line represents the average S_{hmin} gradient of the Rieth-1 and Natarp-1 boreholes. Dark grey shows single standard deviation (68.3 % of normally distributed values) and light grey shows triple standard deviation (99.7 % of normally distributed values).

5.2 Influence of Faults and Saddle Structures

The influence of major faults like the Cappenberg fault (Fig. 5) in Haus Aden on the stress field was tested using data from four boreholes (two vertical and two horizontal) at 1000 m depth [4]. The results indicate that the boreholes (B1/H, B2/V) in the hanging wall exhibit higher stresses than those in the footwall block (B4/V, B2/H) or nearby saddle structure, regardless of whether the boreholes are horizontal or vertical. We excluded the data of these measurement locations due to the potential influence of the fault structure and the large error bar of B2/V.

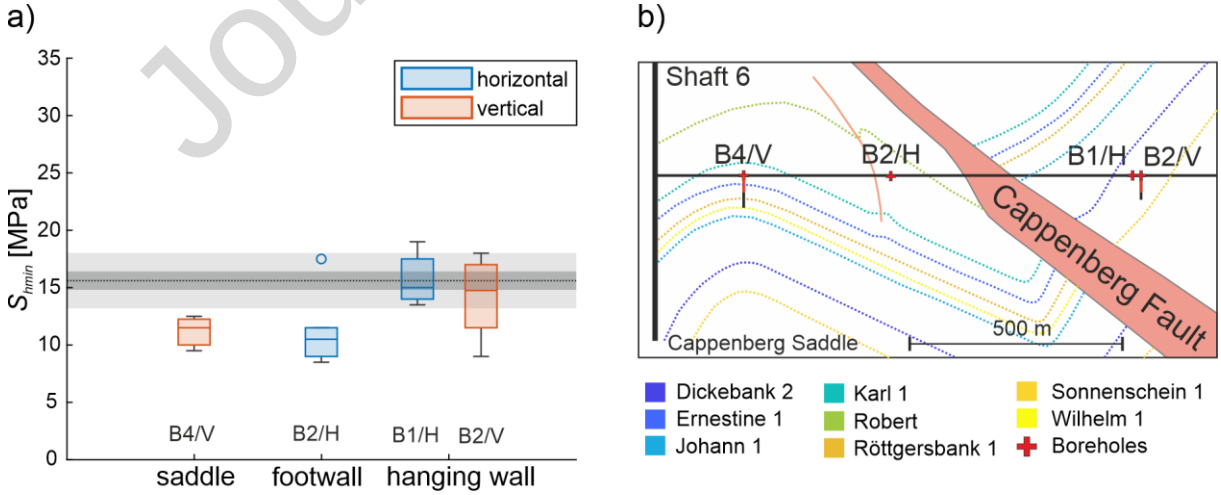

Fig. 5: a) Box plots showing S_{hmin} stress magnitudes in wells B4/V, B2/H, B1/H, and B2/V, categorized by their location (saddle, footwall, and hanging wall). Horizontal wells are

shown in blue and vertical wells are shown in red. The dashed line represents the average S_{hmin} magnitude of the Rieth-1 and Natarp-1 boreholes. Dark grey shows single standard deviation (68.3 % of normally distributed values) and light grey shows triple standard deviation (99.7 % of normally distributed values). b) N-S profile illustrates the Cappenberg Saddle and adjacent Cappenberg thrust fault with the four boreholes at 1000 m depth as well as the seam positions based on [4].

5.3 Influence Distance to Gallery

Stresses near excavations are influenced by stress concentrations and changes in the rheologic properties of the rock (see chapter 2.2). Despite considerable uncertainty, the S_{hmin} gradients increase with distance from the gallery for boreholes in Haus Aden and Westfalen (Fig 6). The comparison with the independent measurements in the deeper boreholes outside the mining area show good agreement for distances > 20 m to the gallery. We follow the suggestion by [3] and exclude measurements closer than 20 m to the galleries for the determination of the regional stress field.

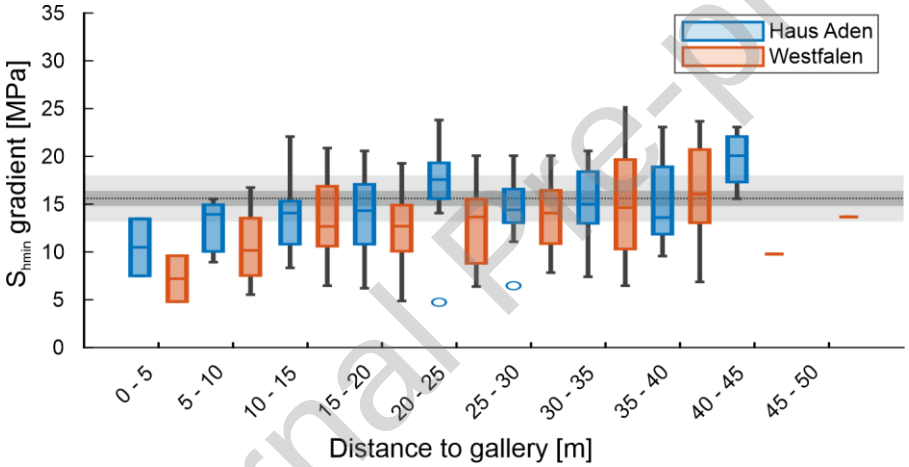

Fig. 6: Plot of the S_{hmin} gradients from the compilation of all published data in the Haus Aden and Westfalen mines based on their distance from the mine shaft. The dashed line represents the average S_{hmin} gradient of the Rieth-1 and Natarp-1 boreholes. Dark grey shows single standard deviation (68.3 % of normally distributed values) and light grey shows triple standard deviation (99.7 % of normally distributed values).

5.4 Influence of undercut sections and lateral distance to mining activities

In the Northfield of the Haus Aden mine four boreholes were drilled and tested in different times enabling the evaluation of undercut mining on the stress field. The boreholes 1229V and 1231H were drilled from the depth level of 750 m and were tested after the lower 880 m depth level has been excavated [5]. Thus, the 750 m depth is the undercut level and has been destressed. Combining the hydraulic fracturing test date information from all of the boreholes at Haus Aden with the mining dates based on “Bürgerinformationsdienst der RAG - BID” [80], it is evident that no other hydraulic fracturing test was conducted above, below or near the active mine. Accordingly, a comparison is made between the stress magnitudes of the two boreholes with the stress magnitudes of the boreholes 1165V and 1166H, which are in the direct vicinity but were measured prior to the excavation of the 880-meter level (Fig. 7).

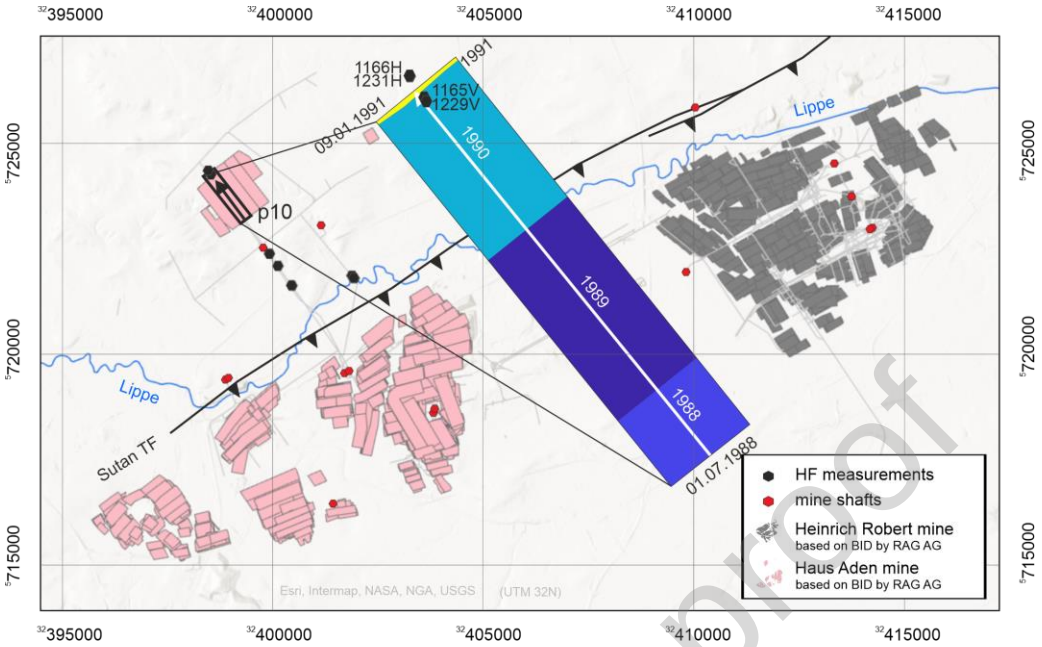

Fig. 7: Location of the hydraulic fracturing measurements in the Haus Aden mine with respect to mining work and mine-shafts. The mining field p10 north of the Sutan thrust fault (TF: based on Allgaier et al., 2024), with the hydraulic fracturing measurements in the boreholes 1165V, 1166H, 1229V and 1231H is enlarged in the center. Colors show the mean year in which the segments were mined [80].

The first mined field in the northern part of Haus Aden mine was the field p10. It was mined from SE to NW. The HF measurements on the 750 m level were performed in September 1989 in the boreholes 1165V and 1166H. During that time none of the neighboring fields were mined. The main mining activity near the HF test sites took place in the year 1990 and in the first days of 1991 (until 09.01.1991) at a depth of 880 m, which is around 130 m below the level of the HF tests. After the minefield p10 was completely mined the boreholes 1229V and 1231H were tested in April 1991.

The comparison of the stress magnitudes shows the difference between the undercut and non- undercut situation (Fig. 8). The stress magnitudes determined after undercut-mining show a significant reduction of the S_{hmin} gradients. In the vertical boreholes the average gradients decrease from 19.3 MPa/km to 10.4 MPa/km. In the horizontal boreholes the decrease is from 16.5 MPa/km to 11.1 MPa/km. As a consequence, the data where undercut-mining could have influenced the measurement should be excluded from stress field analysis.

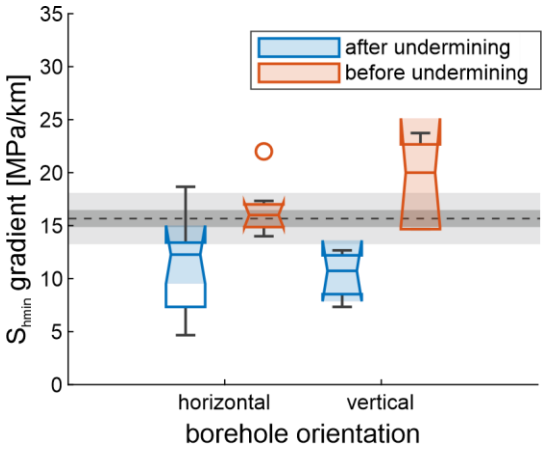

Fig. 8: The S_{hmin} gradients of measurements in boreholes of Haus Aden at the 750 m level show lower stresses for the undercut (destressed) situation in comparison to the earlier measurements where the 750 m level has not been undercut. The dashed line represents the average S_{hmin} gradient of the Rieth-1 and Natarp-1 boreholes. Dark grey shows single standard deviation (68.3 % of normally distributed values) and light grey shows triple standard deviation (99.7 % of normally distributed values).

In the Westfalen mine, boreholes B1/V and B2/H were subsequently undercut. However, the HF test sites are at a distance of several hundred meters to the active mining during the HF test period, suggesting that they remained unaffected. The boreholes B9/H and B10/V are located outside the direct mining area, but within the pillars of adjacent mine workings (approximately 50-80 m away, by comparison of BID database for mining sequence and HF test periods) which were mined at several levels during the HF test period and which could be affected by stress arching and mining activities which leads to very high S_{hmin} in B9/H and low S_{hmin} in B10/V. Consequently, these boreholes should be also excluded from the stress analysis.

5.5 Influence of Borehole Orientation and Fracture Orientation on the Determination of Stresses

The HF method allows for the measurement of a single stress component, but not the complete stress tensor. By increasing the pressure within the packer interval, fractures are typically generated perpendicular to the minimum stress orientation. The orientation therefore strongly depends on the stress regime. In thrust faulting, the minimum stress is S_V, while in strike-slip and normal faulting, the minimum stress is the smaller principal horizontal stress and thus S_{hmin} is determined. According to the results of the deep drillholes Rieth-1 and Natarp-1 the tectonic regime is a normal faulting regime.

In order to obtain reliable results from HF measurements, it is recommended that only boreholes with borehole axes parallel to one of the principal stresses be tested [81]. Thus, shear stresses and non-planar hydraulic fractures in the vicinity of the wellbore (see also Fig. 1 in [82]), which have an impact on the breakdown pressure, can be avoided. As the orientation of the horizontal boreholes is sometimes not given or strongly varying, and mostly not parallel to one of the principal stresses, the results of HF from horizontal wells have been excluded in our study.

6 Results of the Re-Evaluation of Stress Magnitude and Pore Pressure Data in Mines

For this study, we have selected the data that are not influenced by mining activities to derive stress magnitudes. For the derivation of S_V magnitudes, we have interpreted litho-density logs and lithology-data from 14 wells (supplement 6). In comparison to previous interpretations, we considered the pore pressure to determine S_{Hmax} magnitude, and for the pore pressure deduction we have examined the mineralization of the mine waters (supplement 3).

According to the above described selection we use a reduced amount of data which we also checked for plausibility: a) the derived magnitudes and gradients of S_{Hmax} should be higher than those of S_{hmin} and b) we used only those results with S_{hmin} gradients that fit within a range defined by 3 times the standard deviation of the results of the deep nearby boreholes Rieth-1 and Natarp-1, i. e. in the range 13.2-18.0 MPa/km.

The filtered HF data result in a S_{hmin} gradient of 14.9±1.3 MPa/km and 14.4±1.3 MPa/km for Haus Aden and Westfalen, respectively (supplement 9). To derive the S_{Hmax} gradient, knowledge of pore pressure is essential (supplement 5). As described above pore pressure is rather unclear in the Haus Aden and Westfalen mines. Therefore, the S_{Hmax} gradient could range from 25.4 (Westfalen) to 26.2 MPa/km (Haus Aden) for a pore pressure of zero and range from 15.8 MPa/km (Westfalen) to 16.3 (Haus Aden) MPa/km for a pore pressure gradient of 10.4 MPa/km.

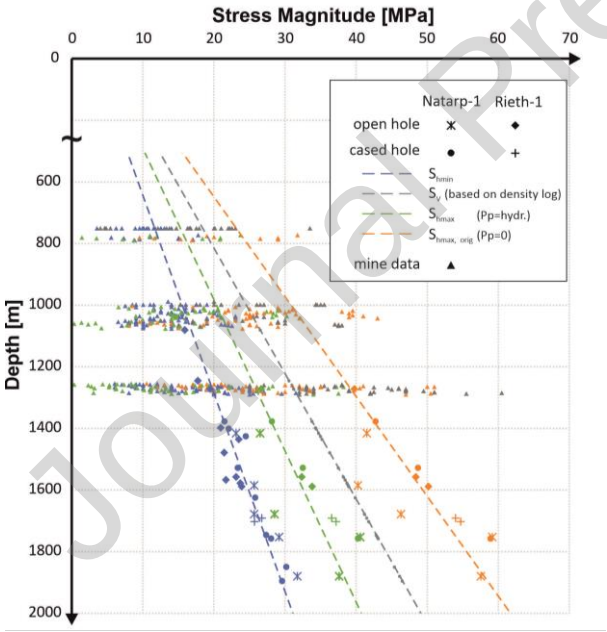

Fig. 9: Measured S_{hmin} stress magnitudes and calculated S_{Hmax} and S_V magnitudes. S_{Hmax} magnitudes are displayed as original data which had been calculated under the assumption of zero pore pressure [83-85] provided in [72] and as S_{Hmax} magnitudes calculated under the assumption of hydrostatic pore pressure (this study). A linear regression has been performed on each series of data (dashed line) to derive stress gradients. In addition, the stress magnitudes from the HF tests in mines are added as triangles.

7 Discussion

To investigate whether stress data from mining can be used to determine the regional stress field, the data were filtered and compared to a reference data set. Two boreholes, Rieth-1 and Natarp-1, located near the mines Haus Aden and Westfalen (Fig. 3) were used as references. The distance between the two boreholes and between boreholes and mine is far enough to assume that there is no resultant stress-interaction between boreholes and mine. Measurements in both boreholes exhibited consistent stress gradients which further support that these measurements reflect the in-situ stress state. Within the mining areas several effects can alter the stress field. Their impact was assessed to reduce uncertainty. However, as the stress field is often the superposition of several effects, extracting the impact of a single effect can provide additional information e.g. on the stress regime or the pore pressure. Several local influences on the observed stress data such as lithology (Fig. 4) and nearby fault and fold structures (Fig. 5), stress concentration and distance to the mine gallery (Fig. 6) and the effects of undercut-mining (Figs. 7, 8) and borehole orientation, had been identified and used for interpreting the data from the mining activity. Apart from these influences there are uncertainties in the test procedure itself, especially with regard to the reopening pressure P_r. The reopening pressure directly affects the determination of the maximum horizontal stress and depends on the compliance of the test equipment and injection rates. The effect of the reopening pressure uncertainty on the S_{Hmax} derivation is described in Supplement 5.

The geology of the Ruhr area is characterized by significant normal faults, such as the Flierich and Koenigsborner Faults, with displacements of several hundred meters [86]. Faults with large displacements often induce rotations in stress orientations and alter stress magnitudes by juxtaposing weaker against stronger rock units. The Cappenberg Fault (Fig. 5), a former thrust fault with up to 200 meters of displacement [4], also exhibits reduced stress magnitudes in the footwall north of the fault compared to reference data, while the hanging wall remains unaffected. Whether the hanging or footwall is affected by stress reduction depends on the prevailing stress regime [87]. As a consequence, the observed stress reduction in the footwall of the fault, compared to the hanging wall stresses probably indicate a prevailing normal faulting regime in the Ruhr area. This is further supported by the stress regime obtained from Rieth-1 and Natarp-1 well data. To investigate the spatial extent of the stress re-orientation, detailed numerical models are required, which are beyond the scope of this wok. However, from generic numerical models, the zone of influence of nearby faults can be calculated up to 2 km [87]. Nevertheless, the larger stress changes are located mainly within the first few hundred meters in the immediate vicinity of large faults [87]. The influence of minor faults or fractures on the stress field is smaller [88]. For longwall mining operations, large displacements along faults are a challenge and stress concentrations in their vicinity are known. Therefore, in the Ruhr area, a distance of several hundred meters has been maintained from major faults for the determination of the regional stress field. If measurements are made within the mines, no influence of major faults are expected. In contrast, drifts can cross these faults. Often HF tests are performed within boreholes drilled from galleries e.g. the HF tests in the Haus Aden mine. There it is of particular importance to consider the location of faults and folds, as well as the distance of the HF test to them.

Furthermore, the occurrence of stress concentrations and stress disturbances is well-known around underground excavations. Here an increased vertical stress is expected on the sides of excavations, whereas a reduced vertical stress results at their top and bottom (stress

arching). These altered stresses can exceed the rock strength, leading to the formation of an excavation damage zone (EDZ) characterized by reduced rock strength and stress magnitudes. The extent of these zones is often estimated based on circular openings using the Kirsch equation [41]. However, the shape of the excavation and orientation significantly influences the horizontal or vertical extent of an EDZ, particularly in an anisotropic stress field [7,47,77,89-91]. At Haus Aden site the shape is rectangular with dimensions of 7.3 m in width and 5.5 m in height [4]. Rectangular tunnel shapes result in higher vertical stresses compared to a circular tunnel [89], likely resulting in the formation of an EDZ with reduced rock strength especially in the vicinity of the corners. The threshold, where disturbed stress observations diminish, and the regional stresses become visible can be approximated by HF tests. Within Haus Aden the S_{hmin} gradients increase with the distance to the gallery, especially within the first 15 m . However, the definition of a precise threshold based on HF test results alone is challenging due to large uncertainties. However, integrating rock strength and fracture analysis from the boreholes B1/H, B2/V, B3/H, and B4/V at Haus Aden mine indicate a threshold of 20 m, which is the distance where Kück [77] identified stress and tensile strength maxima along with constant microfracture length and fracture distribution. Subsequent studies [4,66] also used this 20 m as a threshold for HF tests in Haus Aden. However, Rummel noted that the zone of stress concentration might extend to a greater distance [3]. This is partly supported by observations at Haus Aden, which seem to indicate that increased stress magnitudes can also occur at a distance of 20-25 m, compared to shallower and deeper borehole sections. Due to the experimental uncertainties, these findings lack statistical significance. In this study, the threshold was set to 20 m, as deviations from undisturbed stress conditions beyond this distance are minimal, at least for S_{hmin}. As noted earlier, S_{Hmax} cannot be measured directly, and its determination carries greater uncertainty compared to S_{hmin}. Due to the lack of data, the extent of disturbed S_{Hmax} may be larger, potentially requiring a higher threshold. A similar trend in S_{hmin} is observed at Westfalen mine (Fig. 6). This suggests that the results from Haus Aden can be applied to Westfalen mine as well. No significant correlation of S_{hmin} gradients and lithology was observed. However, lower values are observed for fractured rocks. Data from these tests are excluded as they violate the HF test requirement of an impermeable borehole wall. For fractured rocks HTPF tests [92] or PSI-methods [93,94] should be utilized.

In this study, all HF-measurements in horizontal boreholes were excluded, as only boreholes with their borehole axes parallel to one of the principal stresses provide reliable results [81]. This assumption is reasonable for vertical boreholes at greater depths and in areas without significant topography [95], which is the case in the eastern Ruhr area. Therefore, the likelihood of inducing shear stresses that could affect the breakdown pressure is minimal. In horizontal boreholes, shear stresses may be induced if the borehole axis is not perfectly aligned with one of the principal horizontal stress orientations, potentially leading to altered stress magnitudes. However, if a horizontal borehole axis is aligned parallel to the S_{Hmax} orientation and if a vertical fracture parallel to the borehole axis is created during the HF test, the vertical stress can be determined. As shown, the HF test can be influenced by several factors that affect the magnitude of stress, particularly in mining areas. This is reflected in the generally high standard deviations of the results for S_V. Therefore, the more robust method of integrating density logs (Figs. S.6.2 and S. 6.3) is used to derive vertical stress in this study. The regional S_V gradient of deep boreholes (unaffected by the mining) range for the gradient of S_V =24.3-24.6 MPa/km. However, for two boreholes, B2/H and B12/H, it was possible to eliminate most of the external factors except pore pressure. These boreholes, drilled in compact sandstone, showed consistent S_{hmin} values with values measured with a threshold of 20 m from the gallery.

Additionally, for determination of S_V and S_{Hmax} precise pore pressure information is required. Pore Pressure is typically assessed using hydraulic pressure fall-off tests, such as Drill-Stem-Tests, or by the integration of fluid mineralization data from deep boreholes. Regional data from the Rieth-1 and Natarp-1 borehole suggest a slightly over-hydrostatic pore pressure of 10.4 MPa/km (Fig. S.3.2). It needs to be taken into account that local conditions in the vicinity of mines may differ. Historical reports on pore pressure are often inconsistent and incomplete, making it difficult to accurately derive S_{Hmax}. Assuming zero pore pressure in mines and their surroundings, as in most of the earlier reports [5,21,79,83-85,96], may result in an overestimation of the S_{Hmax}, while assuming full hydrostatic pore pressure conditions may lead to underestimation of S_{Hmax}. In mining areas, the assumption of a generally hydrostatic pore pressure is often unjustified due to centuries of mining combined with the extensive dewatering to enable mining works. The generally low matrix permeability of Carboniferous rocks [73] suggests that locally full hydrostatic pressure may be present already a few meters from the mine opening and outside the excavation damage zone (where reduced or near zero pore pressure could prevail, due to the fractured character with enhanced permeability). At Haus Aden mine, non-zero pore pressures were observed in some of the permeability tests conducted as part of the HF tests (supplement 4) [3,77]. These tests were carried out in galleries distant from active mining. Thus, it is possible that these parts of the mines and the surrounding area were not fully dewatered at the time of the measurements. In contrast, in the immediate vicinity of the mining levels, the pore pressure is reduced to almost zero, especially if the mining activity has been ongoing for already several decades. However, no specific pore pressure measurements, such as drill-stem tests, have been conducted in these mine boreholes, leaving pore pressure estimates uncertain between zero and hydrostatic conditions.

To address this uncertainty, we used an inverse approach for the two boreholes, B2/H and B12/H, which are assumed to be only affected by pore pressure reduction. We set the vertical stress to the reference value obtained from density log integration. For correct results we included the depth of the Carboniferous surface, obtained from www.geoportal-nrw.de, at the measurement sites in the calculations of $S_{V\,\mathrm{ref}}$. The pore pressure was approximated as the difference between the zero pore pressure solution $S_{V\,(Pp=0)}$ and the reference value $S_{V\,\mathrm{ref}}$. Backward calculations of pore pressure in both boreholes confirmed a decrease in pore pressure near to the gallery. In B12/H, the pore pressure was reduced by approx. 75% and persisted up to 39 m (maximum depth of borehole) from the gallery. In contrast, B2/H showed a smaller reduction (57 %) with a significant increase in pore pressure towards the bottom of the borehole, approaching nearly hydrostatic conditions (Table S.10).

This highlights the heterogeneity of pore pressure distribution even within in the same mine, emphasizes the uncertainty of calculating S_{Hmax} or S_V from HF tests without accurate pore pressure data. It was found that pore pressure ranges from nearly zero to full hydrostatic. Assuming zero pore pressure, the average horizontal stress gradients for the Haus Aden mine and Westfalen mine would be S_{Hmax}: 25.8 MPa/km, S_{hmin}: 14.65 MPa/km, Pp: 0 MPa/km. Assuming a hydrostatic pore pressure gradient of Pp = 10.4 MPa/km, S_{Hmax} decreases to 16.1 MPa/km. According to supplement 5 the pore pressure reveals much higher uncertainties for the derivation of SHmax in comparison to e.g. the reopening pressure.

Earlier published studies using mining data of the Haus Aden mine, which report S_V = 24.4-26.4 MPa/km, S_{Hmax} = 25.5-35.5 MPa/km, S_{hmin} 13.6-17.3 MPa/km [68] based on [97], and thus a strike slip tectonic regime. A more recent publication reported stress gradients of S_V: 24.4 MPa/km, S_{Hmax}: 28.1 MPa/km, S_{hmin}: 14.5 MPa/km [21] based on [72], which is consistent with the findings of this study, when assuming zero pore pressure. In this publications pore pressure is either not specified [68] or variable. In the original reports, negligible pore pressure was assumed, except for Haus Aden B1-B4 (supplement 8). Despite these differences, all studies suggest a strike-slip tectonic regime.

The same strike -slip regime is reported by a study including data from the broader Ruhr area, with an reported S_V gradient of 23.1 ± 1.3 MPa/km, an S_{hmin} gradient of 16.1 ± 4.3 MPa/km and an S_{Hmax} gradient of 33.6 ± 9.6 MPa/km [98]. The lower average vertical stress results from the inclusion of data from the northwest of our study area, where a thicker Cretaceous unit with lower density (Supplement 6) overlays the Carboniferous rocks. This study also reports a pore pressure gradient of 10.8 ± 1 MPa/km, which is slightly higher than the 10.4 MPa/km determined in this study. This, for the results insignificant difference, can be attributed to the broader depth range of the analyzed samples. Shallower water typically has lower mineralization than deeper sections, which directly affects average fluid densities (Supplement 3).

In contrast, S_{Hmax} magnitudes from the two deep boreholes (Rieth-1 and Natarp-1), differ significantly from those deducted within the mines and from published studies, although S_{hmin} and S_V are within the same range. These data are much more uniform, indicating a normal faulting tectonic regime with S_V: 24.5 MPa/km, S_{Hmax}: 21.0 MPa/km, S_{hmin}: 15.5 MPa/km, consistent with previous reports [4,66]. The S_{Hmax} gradient from the deep boreholes is between the gradients obtained in the mine with and without pore pressure, indicating that the pore pressure in mines is neither zero nor hydrostatic (Supplement 10).The prevailing normal faulting regime in the Eastern Ruhr area is further supported by HF tests in the vicinity of the Cappenberg Fault and their interpretation by numerical modelling [87]. The observed reduction in stress magnitude in the footwall can indicate a prevailing normal faulting tectonic regime in the vicinity of the fault but does not support the assumption of a strike slip regime as obtained with mine data and while assuming zero pore pressure.

The state of stress is closely linked to seismicity. A common method for assessing the fault reactivation potential, and thus seismicity, is the slip tendency of faults [99]. This approach has been used in several studies to evaluate the seismic risk of the Ruhr area [21,65,66,100]. In studies where a strike slip regime was assumed, most of the faults were found to be critically stressed, increasing the likelihood of natural seismicity.

The western Ruhr area may exhibit strike-slip tectonics, as indicated by earthquake focal mechanisms demonstrating strike-slip behavior. In contrast, the eastern Ruhr area exhibits low levels of natural seismic activity [64]. Observed seismic events in this region are primarily linked to mining operations [101,102], implying a comparatively less critical stress state. This observation is consistent with previous studies that support a normal faulting regime for the region [66].

8 Conclusions and Outlook

We conducted an analysis using different filtering methods to mitigate the effect of stress perturbations caused by mine opening and mining operations or extract single effects to get additional information e.g. on pore pressure or the tectonic regime. Our analysis reveals significant variability in S_{hmin} magnitudes within the mines, whereas more uniform results were obtained from two nearby deep boreholes (Rieth-1 and Natarp-1), which are unaffected by stress perturbations.

Independent from lithology our analysis shows that a high degree of rock fracturing correlates with lower Shut In pressures because the pressure is not only penetrating the impermeable borehole wall but also the fracture surfaces. These data cannot be used to determine the regional stress field and must be excluded from further analysis.

A key finding is that most HF test data from mine levels and galleries do not represent the regional stress state. Instead, they are heavily influenced by mine geometry, proximity to faults and folds, and the temporal evolution of the mine (undercut mining) and need to be excluded for regional stress determinations.

Pore pressure, crucial for calculating effective magnitudes of S_V, S_{hmin} and S_{Hmax}, is often poorly known in mining environments, introducing substantial uncertainty in determining of those stress components, which cannot be measured directly. This uncertainty can lead to an altered tectonic stress regime, changing strike slip faulting to normal faulting regime. Because of lacking pore pressure information within the mines, we determined the regional stress field based on the two deep boreholes, where hydraulic fall-off tests were available (S_V: 24.5 MPa/km, S_{Hmax}: 21.0 MPa/km, S_{hmin}: 15.5 MPa/km, Pp: 10.4 MPa/km).

Our recommendations for the derivation of regional stress from HF data in mines are:

a) to use only those HF data from locations where pore pressure information is available at the time of testing to determine the S_{Hmax} magnitude,

b) to handle HF data measured close to excavations (galleries and mining areas) with caution, as they have limited relevance for broader applications, like creating of regional stress maps (e.g. the World Stress Map [8]), without additional information about the mining process (timing, design of the mine),

c) For HF fracturing in mines and tunnels we suggest applying similar quality ranking criteria as used in the WSM for overcoring [6,17,103]. This would improve their use as regional stress indicators. Such a quality ranking could for example require to have exact borehole orientations, orientation of the generated fractures, pore pressures, timing and design of the mine. If independent information from deep nearby boreholes is available and confirms the mining data, it should be considered in the quality assessment.

CRediT authorship contribution statement

Thomas Niederhuber: Conceptualization, Data curation, Formal analysis, Investigation, Methodology, Visualization, Writing – original draft, Writing – review and editing

Martina Rische: Conceptualization, Formal analysis, Investigation, Methodology, Writing – original draft, Writing – review and editing

Birgit Müller: Conceptualization, Formal analysis, Funding acquisition, Investigation, Methodology, Supervision, Writing – original draft, Writing – review and editing

Thomas Röckel: Conceptualization, Formal analysis, Investigation, Methodology, Validation, Writing – original draft, Writing – review and editing

Felix Allgaier: Writing – original draft, Writing – review and editing

Kasper Fischer: Funding acquisition, Supervision, Writing – review and editing

Frank Schilling: Supervision, Resources, Software, Writing – review and editing

Wolfgang Friederich: Funding acquisition, Project administration, Resources, Software, Supervision, Writing – review and editing

Funding sources

This work was carried out in scientific cooperation with GD NRW and ALBER Geomechanics as part of the FloodRisk project (grants FKZ:03G0893 A-E) funded by GEO:N a funding program sponsored by the German Federal Ministry of Education and Research.

Acknowledgments

We thank all project partners for their invaluable expert advice and contributions. A special thanks to RAG for their support in releasing and providing the necessary data for our research. We would also like to thank Gerd Klee of Solexperts for his expert advice and Jochem Kück for his clarification of the hydraulic fracturing data used in previous studies.

Open Research Section

Geologischer Dienst NRW. IS RK 10 KO DS - Informationssystem Geologische Karte des Rheinisch-Westfälischen Steinkohlengebietes 1:10 000 (Datensatz). http://www.gis-rest.nrw.de/atomFeed/rest/atom/08997aa6-7257-4906-9887-0c63744a9242/d04a7b1e-3e60-4591-b04c-94912ac54afe.html

References

1. Hast N. The state of stresses in the upper part of the earth's crust. *Engineering Geology*. 1967;2(1):5-17. doi:10.1016/0013-7952(67)90002-6.
2. Scheidegger AE. Stress in earth's crust as determined from hydraulic fracturing data. *Geologie und Bauwesen*. 1962;27(2):45-53.
3. Rummel F. *Abschlussbericht Hydrofrac-Spannungsmessungen in der Schachtanlage 'Haus Aden'*. [RUB-Az.: O.N.]; 1986.
4. Stelling W, Rummel F. Messung von Primärspannungen durch Hydraulik-Fracturing auf dem Bergwerk Haus Aden. *Das Markscheidewesen*. 1992;99(1):176-184.
5. Müller W. The stress state in the Ruhr coalfield. In: *Berichte: 7. Internationaler Kongress über Felsmechanik Aachen, Deutschland, [16. - 20. September]*. Rotterdam: Balkema; 1991:1707-1711; 3.
6. Zoback ML, Zoback MD, Adams J, et al. Global patterns of tectonic stress. *Nature*. 1989;341(6240):291-298. doi:10.1038/341291a0.
7. Amadei B, Stephansson O. *Rock stress and its measurement.* 1. ed. London, Weinheim: Chapman & Hall; 1997.
8. Heidbach O, Rajabi M, Reiter K, Ziegler M. *World Stress Map 2016*. GFZ Data Services; 2016.
9. Morawietz S, Heidbach O, Reiter K, et al. An open-access stress magnitude database for Germany and adjacent regions. *Geotherm Energy*. 2020;8(1). doi:10.1186/s40517-020-00178-5.
10. Heidbach O, Barth A, Müller B, et al. *WSM quality ranking scheme, database description and analysis guidelines for stress indicator*. GFZ German Research Centre for Geosciences; 2016.
11. Fritschen R. Mining-Induced Seismicity in the Saarland, Germany. *Pure appl geophys*. 2010;167(1-2):77-89. doi:10.1007/s00024-009-0002-7.
12. Blake W, Hedley DGF. *Rockbursts: Case studies from North American hard-rock mines.* 1st ed; 2003.
13. Ritter W. *Statik der Tunnelgewölbe*. Berlin: J. Springer; 1879.
14. Ting CH, Shukla SK, Sivakugan N. Arching in Soils Applied to Inclined Mine Stopes. *Int J Geomech*. 2011;11(1):29-35. doi:10.1061/(ASCE)GM.1943-5622.0000067.
15. Huang X, Ruan H, Shi C, Kong Y. Numerical Simulation of Stress Arching Effect in Horizontally Layered Jointed Rock Mass. *Symmetry*. 2021;13(7):1138. doi:10.3390/sym13071138.
16. Wang F, Chen T, Ma B, Chen D. Formation mechanism of stress arch during longwall mining based on key strata theory. *Energy Exploration & Exploitation*. 2022;40(2):816-833. doi:10.1177/01445987211042701.
17. Zoback ML. First-and second-order patterns of stress in the lithosphere: The World Stress Map Project. *Journal of Geophysical Research: Solid Earth*. 1992;97(B8):11703-11728. doi:10.1029/92JB00132.
18. Stephansson O, Ångman P. Hydraulic fracturing stress measurements at Forsmark and Stidsvig, Sweden. *Bulletin of the Geological Society of Finland*. 1986;58(Part 1):307-333.

19. Liu C. Distribution Laws of in-Situ Stress in Deep Underground Coal Mines. *Procedia Engineering*. 2011;26:909-917. doi:10.1016/j.proeng.2011.11.2255.
20. Sandström D. *Analysis of the virgin state of stress at the Kiirunavaara mine. 1402-1757*. 2003. Licentiate thesis / Luleå University of Technology.
21. Kruszewski M, Klee G, Niederhuber T, Heidbach O. In situ stress database of the greater Ruhr region (Germany) derived from hydrofracturing tests and borehole logs. 2022. doi:10.5194/essd-2022-196.
22. Niederhuber T, Kruszewski M, Röckel T, Rische M, Alber M, Müller B. Stress orientations from hydraulic fracturing tests in the Ruhr area in comparison to stress orientations from borehole observations and earthquake focal mechanisms. *Z. Dt. Ges. Geowiss. (J. Appl. Reg. Geol.),*. 2023;173(4):625-635. doi:10.1127/zdgg/2022/0352.
23. GD NRW. *Grßtektonik Ruhrgebiet*. Krefeld, Germany: Geologischer Dienst Nordrhein-Westfalen - geodaten; 2017. http://www.gis-rest.nrw.de/atomFeed/rest/atom/3b81e661-ac40-44f9-ab8a-93a8bed8b620.html. Accessed August 14, 2024.
24. Bourne SJ. Contrast of elastic properties between rock layers as a mechanism for the initiation and orientation of tensile failure under uniform remote compression. *J Geophys Res*. 2003;108(B8). doi:10.1029/2001JB001725.
25. Teufel LW. *Influence of lithology and geologic structure on in situ stress: examples of stress heterogeneity in reservoirs*. Albuquerque, NM (United States); 1989; SAND-89-1435C; CONF-890620-1; ON: DE89014692.
26. Warpinski NR, Teufel LW. In-Situ Stresses in Low-Permeability, Nonmarine Rocks. *Journal of Petroleum Technology*. 1989;41(04):405-414. doi:10.2118/16402-PA.
27. Evans KF, Engelder T, Plumb RA. Appalachian Stress Study: 1. A detailed description of in situ stress variations in Devonian shales of the Appalachian Plateau. *J Geophys Res*. 1989;94(B6):7129-7154. doi:10.1029/JB094iB06p07129.
28. Plumb RA, Evans KF, Engelder T. Geophysical log responses and their correlation with bed-to-bed stress contrasts in Paleozoic rocks, Appalachian Plateau, New York. *J Geophys Res*. 1991;96(B9):14509-14528. doi:10.1029/91JB00896.
29. Hergert T, Heidbach O, Reiter K, Giger SB, Marschall P. Stress field sensitivity analysis in a sedimentary sequence of the Alpine foreland, northern Switzerland. *Solid Earth*. 2015;6(2):533-552. doi:10.5194/se-6-533-2015.
30. Reiter K. Stress rotation – impact and interaction of rock stiffness and faults. *Solid Earth*. 2021;12(6):1287-1307. doi:10.5194/se-12-1287-2021.
31. Turcotte DL, Schubert G. *Geodynamics.* 2. ed. Cambridge: Cambridge Univ. Press; 2002. http://www.loc.gov/catdir/description/cam021/2001025802.html.
32. Warpinski NR, Teufel LW. In situ stress measurements at Rainier Mesa, Nevada test site—Influence of topography and lithology on the stress state in tuff. *International Journal of Rock Mechanics and Mining Sciences & Geomechanics Abstracts*. 1991;28(2-3):143-161. doi:10.1016/0148-9062(91)92163-S.
33. Shamir G, Zoback MD. Stress orientation profile to 3.5 km depth near the San Andreas Fault at Cajon Pass, California. *J Geophys Res*. 1992;97(B4):5059-5080. doi:10.1029/91JB02959.

34. Barton CA, Zoback MD. Stress perturbations associated with active faults penetrated by boreholes: Possible evidence for near-complete stress drop and a new technique for stress magnitude measurement. *J Geophys Res*. 1994;99(B5):9373-9390. doi:10.1029/93JB03359.
35. Mariucci MT, Amato A, Gambini R, Giorgioni M, Montone P. Along-depth stress rotations and active faults: An example in a 5-km deep well of southern Italy. *Tectonics*. 2002;21(4). doi:10.1029/2001TC001338.
36. Sahara DP, Schoenball M, Kohl T, Müller B. Impact of fracture networks on borehole breakout heterogeneities in crystalline rock. *International Journal of Rock Mechanics and Mining Sciences*. 2014;71:301-309. doi:10.1016/j.ijrmms.2014.07.001.
37. Sonder LJ. Effects of density contrasts on the orientation of stresses in the lithosphere: Relation to principal stress directions in the Transverse Ranges, California. *Tectonics*. 1990;9(4):761-771. doi:10.1029/TC009i004p00761.
38. Ziegler MO, Seithel R, Niederhuber T, et al. The effect of stiffness contrasts at faults on stress orientation. 2024. doi:10.5194/egusphere-2024-1109.
39. Martin CD. Seventeenth Canadian Geotechnical Colloquium: The effect of cohesion loss and stress path on brittle rock strength. *Can Geotech J*. 1997;34(5):698-725. doi:10.1139/t97-030.
40. Kaiser PK, Yazici S, Maloney S. Mining-induced stress change and consequences of stress path on excavation stability — a case study. *International Journal of Rock Mechanics and Mining Sciences*. 2001;38(2):167-180. doi:10.1016/S1365-1609(00)00038-1.
41. Kirsch EG. Die Theorie der Elastizit t und die Bed rfnisse der Festigkeitslehre. *Zeitshrift des Vereines deutscher Ingenieure*. 1898;42:797-807.
42. Kelsall PC, Case JB, Chabannes CR. Evaluation of excavation-induced changes in rock permeability. *International Journal of Rock Mechanics and Mining Sciences & Geomechanics Abstracts*. 1984;21(3):123-135. doi:10.1016/0148-9062(84)91530-4.
43. Albers HJ. Konventioneller Ausbau und die Neue Österreichische Tunnelbauweise im Steinkohlenbergbau. *Glückauf*. 1985;121(11):833-839.
44. Wittke W. Tunnel und Stollen. In: Wittke W, ed. *Felsmechanik*. Berlin, Heidelberg: Springer Berlin Heidelberg; 1984:419-506.
45. Whittaker BN. An appraisal of Strata control practice. *Mining Engineer*. 1974:9-24.
46. McGarr A. Seismic moments and volume changes. *J Geophys Res*. 1976;81(8):1487-1494. doi:10.1029/JB081i008p01487.
47. Brady BHG, Brown ET. *Rock mechanics for underground mining.* 3. ed. Dordrecht: Springer Science & Business Media; 2004.
48. Trueman R, Pierce M, Wattimena R. Quantifying stresses and support requirements in the undercut and production level drifts of block and panel caving mines. *International Journal of Rock Mechanics and Mining Sciences*. 2002;39(5):617-632. doi:10.1016/S1365-1609(02)00060-6.
49. Bartlett, PJ & Nesbitt, K. Stress induced damage in tunnels in a cave mining environment in kimberlite. *Journal of the Southern African Institute of Mining and Metallurgy*. 2000;100(6):341-345.

50. Drozdzewski GH. The Ruhr coal basin (Germany): structural evolution of an autochthonous foreland basin. *International Journal of Coal Geology*. 1993;23(1-4):231-250. doi:10.1016/0166-5162(93)90050-k.
51. Drozdzewski GH, Hoth P, Juch D, Littke R, Vieth A, Wrede V. The pre-Permian of NW-Germany structure and coalification map. *zdgg*. 2009;160(2):159-172. doi:10.1127/1860-1804/2009/0160-0159.
52. Meschede M, Warr LN. *The Geology of Germany*. Cham: Springer International Publishing; 2019.
53. Driesen B. *Geologische Karte von Nordrhein-Westfalen 1 :100000: Erläuterungen zu Blatt C 4310 Münster*. Krefeld, Germany: GLA NRW; 1990.
54. Rudolph T, Melchers C, Minke A, Coldewey WG. Gas seepages in Germany: Revisited subsurface permeabilities in the German mining district. *Bulletin*. 2010;94(6):847-867. doi:10.1306/10210909074.
55. Kelch H-J. Beschreibung der Spülproben der Kreide der Bohrung Münsterland 1. In: *Die Aufschlussbohrung Münsterland 1.: Ein Symposium.* [568 S., 131 Abb., 64 Tab., 48 Taf.]. Krefeld, Germany: Landesbetrieb; 1963:19-22. *Fortschritte in der Geologie von Rheinland und Westfalen*; 11.
56. Richwein J, Schuster A, Teichmüller R, Wolburg J. Uberblick über das Profil der Bohrung Münsterland 1: Geologische Begründung des Ansatzpunktes S. 9. Stratigraphisches Profil S. II. Geophysik und Diagenese S. 16. In: *Die Aufschlussbohrung Münsterland 1.: Ein Symposium.* [568 S., 131 Abb., 64 Tab., 48 Taf.]. Krefeld, Germany: Landesbetrieb; 1963:9-18. *Fortschritte in der Geologie von Rheinland und Westfalen*; 11.
57. Schäfer A. *Klastische Sedimente.* 2nd ed. Berlin, Heidelberg: Springer Berlin Heidelberg; 2019.
58. Teichmüller M. Die Kohlenflöze der Bohrung Münsterland 1. In: *Die Aufschlussbohrung Münsterland 1.: Ein Symposium.* [568 S., 131 Abb., 64 Tab., 48 Taf.]. Krefeld, Germany: Landesbetrieb; 1963:129-178. *Fortschritte in der Geologie von Rheinland und Westfalen*; 11.
59. Brix MR, Drozdzewski GH, Greiling RO, Wolf R, Wrede V. The N Variscan margin of the Ruhr coal district (Western Germany): structural style of a buried thrust front? *Geol Rundsch*. 1988;77(1):115-126. doi:10.1007/BF01848679.
60. Langefeld O, Paschedag U. Longwall Mining-Development and Transfer. *Mining Report Glückauf*. 2019;155(1):51-72.
61. Drozdzewski GH, Wrede V. Faltung und Bruchtektonik – Analyse der Tektonik im Subvariscikum. *Fort. Geol. Rheinl. Westf.* 1994;38:7-187.
62. Wrede V. Störungstektonik im Ruhrkarbon. *Z. angew. Geol.* 1992;38(2):94-104.
63. Wrede V. Zur Zeitlichkeit postvariscischer Tektonik im südwestlichen Teil des Münsterschen Kreidebeckens. *sdgg*. 2011;73:183-189. doi:10.1127/sdgg/73/2011/183.
64. Grünthal G, Bosse C. *Probabilistische Karte der Erdbebengefährdung der Bundesrepublik Deutschland-Erdbebenzonierungskarte für das Nationale Anwendungsdokument zum Eurocode 8: Scientific Technical Report STR96/10*; 1996.

65. Niederhuber T, Rische M, Röckel T, Müller B, Schilling F. Flooding Induced Seismicity in the Ruhr Area – a geomechanics numerical modelling approach. EGU General Assembly 2023 (24-28.04.2023); 2023; Vienna. https://doi.org/10.5194/egusphere-egu23-15990.
66. Allgaier F, Niederhuber T, Busch B, Müller B, Hilgers C. Post-mining related reactivation potential of faults hosted in tight reservoir rocks around flooded coal mines, eastern Ruhr Basin, Germany. *Geomechanics for Energy and the Environment*. 2024;38:100560. doi:10.1016/j.gete.2024.100560.
67. Huske J. *Die Steinkohlenzechen im Ruhrrevier: Daten und Fakten von den Anfängen bis 2005.* 3., überarb. und erw. Aufl. Bochum: Selbstverl. des Dt. Bergbau-Museum; 2006. Veröffentlichungen aus dem Deutschen Bergbau-Museum Bochum; Nr. 144.
68. Alber M, Fritschen R, Bischoff M, Meier T. Rock mechanical investigations of seismic events in a deep longwall coal mine. *International Journal of Rock Mechanics and Mining Sciences*. 2009;46(2):408-420. doi:10.1016/j.ijrmms.2008.07.014.
69. Schetelig K, Heitfeld M, Rosner P, Paape B. *Gutachten zu den möglichen Auswirkungen eines Grubenwasseranstiegs im Ruhrrevier auf die Schutzgüter und den daraus resultierenden Monitoring-Maßnahmen, im Auftrag der Bezirksregierung Arnsberg, Abteilung 8 Bergbau und Energie in NRW: 198 Seiten, 3 Anh. und 29 Anl;* 2007. https://www.grubenwasser-steinkohle-nrw.de/download?file=223.
70. G.E.O.S. *Abschlussbericht Überprüfung der Aussagen zur Entwicklung der Mineralisation der Grubenwässer im Zuge des Grubenwasseranstieges im nordrheinwestfälischen Steinkohlerevier im Bereich des ehemaligen Bergwerks Ost*. Halsbrücke; 2017.
71. Reiss J. Testarbeiten zum Nachweis von Kohlenwasserstoffen auf der Bohrung Münsterland 1. In: *Die Aufschlussbohrung Münsterland 1.: Ein Symposium.* [568 S., 131 Abb., 64 Tab., 48 Taf.]. Krefeld, Germany: Landesbetrieb; 1963:383-386. *Fortschritte in der Geologie von Rheinland und Westfalen*; 11.
72. Kruszewski M, Klee G, Niederhuber T, Heidbach O. *Reports from Hydrofracturing Tests Performed in the Greater Ruhr Region (Germany) between 1986 and 1995*. Fraunhofer-Gesellschaft; 2022.
73. Greve J, Busch B, Quandt D, Knaak M, Hartkopf-Fröder C, Hilgers C. Coupling heat conductivity and lithofacies of the coal-bearing Upper Carboniferous in the eastern Ruhr Basin, NW Germany. *zdgg*. 2023;173(4):673-695. doi:10.1127/zdgg/2023/0350.
74. Strasser B, Wolters R. Gesteinsmechanische Untersuchungen an Proben aus der Bohrung Münsterland 1. In: *Die Aufschlussbohrung Münsterland 1.: Ein Symposium.* [568 S., 131 Abb., 64 Tab., 48 Taf.]. Krefeld, Germany: Landesbetrieb; 1963:419-446. *Fortschritte in der Geologie von Rheinland und Westfalen*; 11.
75. Creutzburg H. Zur Wärmeleitfähigkeit des paläozoischen Gebirges in der Bohrung Münsterland 1. In: *Die Aufschlussbohrung Münsterland 1.: Ein Symposium.* [568 S., 131 Abb., 64 Tab., 48 Taf.]. Krefeld, Germany: Landesbetrieb; 1963:395-402. *Fortschritte in der Geologie von Rheinland und Westfalen*; 11.
76. DMT. *Abschlussbericht Absolute Spannungsmessungen im Ruhrkarbon im Rahmen bergbaulicher Zuschnittsplanung – Gebirgsspannungen: Bericht EUR 14669 DE*. [Forschungsvertrag Nr. 7220-AF/129]; 1993.

77. Kück J. *Hydraulic fracturing Gebirgsspannungsmessungen auf der 940 m Sohle des Ruhrkohle-Bergwerks 'Haus Aden'*. [Diploma Thesis]. Ruhr-Universität Bochum; 1988.
78. Kruszewski M, Klee G, Niederhuber T, Heidbach O. *In-Situ Stress Magnitude Data from the Greater Ruhr Region (Germany) Derived from Hydrofracturing Tests and Borehole Logs*. Fraunhofer-Gesellschaft; 2022.
79. MeSy. *Compilation of Existing hydrofrac In-Situ Stress Data for the Ruhr Carboniferous: Report No. 28.94*. [internal report in German]; 1994. https://fordatis.fraunhofer.de/bitstream/fordatis/290/8/Compilation_of_existing_hydrofrac_in_situ_stress_data_for_the_ruhr_carboniferous_031_94.pdf.
80. RAG-BID. *Ruhrkohle AG, Bürger Informations Dienst, Grubenwasser Monitoring*. geodaten.rag.de. 2022. https://geodaten.rag.de/mapapps/resources/apps/bid/index.htm. Accessed September 12, 2023.
81. Haimson BC, Cornet FH. ISRM Suggested Methods for rock stress estimation—Part 3: hydraulic fracturing (HF) and/or hydraulic testing of pre-existing fractures (HTPF). *International Journal of Rock Mechanics and Mining Sciences*. 2003;40(7-8):1011-1020. doi:10.1016/j.ijrmms.2003.08.002.
82. Zhang Y, Zhang J, Yuan B, Yin S. In-situ stresses controlling hydraulic fracture propagation and fracture breakdown pressure. *Journal of Petroleum Science and Engineering*. 2018;164:164-173. doi:10.1016/j.petrol.2018.01.050.
83. MeSy. *CBM - Project Sigillaria License Area. Cased-Hole Permeability And Hydrofrac Stress Measurements in Borehole Natrap-1. Final Report: Report No. 39.95*. [internal report in German]; 1995. https://fordatis.fraunhofer.de/bitstream/fordatis/290/2/Cased_hole_permeability_and_stress_measurements_in_borehole_Natrap1_final_report_39_95.pdf.
84. MeSy. *CBM - Project Sigillaria License Area. Cased-Hole Permeability And Stress Measurements in Borehole Rieth-1. Final Report: Report No. 29.95*. [internal report in German]; 1995. https://fordatis.fraunhofer.de/bitstream/fordatis/290/4/Cased_hole_permeability_and_stress_measurements_in_borehole_Rieth1_final_report_29_95.pdf.
85. MeSy. *CBM - Project Sigillaria License Area. Open-Hole Permeability And Hydrofrac Stress Measurements in Borehole Natrap-1. Final Report: Report no. 35.95*. [internal report in German]; 1995. https://fordatis.fraunhofer.de/bitstream/fordatis/290/12/Open_hole_permeability_and_hydrofrac_stress_measurements_in_borehole_Natrap1_Final_Report_35_95.pdf.
86. Kunz E. Tiefentektonik der Emscher- und Essener Hauptmulde im östlichen Ruhrgebiet: dargestellt an der Karbonoberfläche M. 1:100 000. [Tafel 1]. In: *Ergänzende Beiträge zur Tiefentektonik des Ruhrkarbons:* [22 Abb., 3 Tab., 16 Taf.]. Krefeld, Germany: Geologischer Dienst Nordrhein-Westfalen - Landesbetrieb (Verlag); 1988.
87. Reiter K, Heidbach O, Ziegler MO. Impact of faults on the remote stress state. *Solid Earth*. 2024;15(2):305-327. doi:10.5194/se-15-305-2024.
88. Lin W, Yeh E-C, Hung J-H, Haimson B, Hirono T. Localized rotation of principal stress around faults and fractures determined from borehole breakouts in hole B of the Taiwan

Chelungpu-fault Drilling Project (TCDP). *Tectonophysics*. 2010;482(1-4):82-91. doi:10.1016/j.tecto.2009.06.020.
89. Abdellah WR, Ali MA, Yang H-S. Studying the effect of some parameters on the stability of shallow tunnels. *Journal of Sustainable Mining*. 2018;17(1):20-33. doi:10.1016/j.jsm.2018.02.001.
90. Perras MA, Diederichs MS, Lam T. A review of excavation damage zone in sedimentary rocks with emphasis on numerical modelling for EDZ definition. In: Proceedings of the 63rd Canadian Geotechnical Conference; 2010:742-750.
91. Emsley S, Olsson O, Stetenberg L, Alheid H-J, Falls Stephen. *ZEDEX - A study of damage and disturbance from tunnel excavation by blasting and tunnel boring: Technical Report 97-30*; 1997.
92. Cornet FH, Valette B. In situ stress determination from hydraulic injection test data. *J Geophys Res*. 1984;89(B13):11527-11537. doi:10.1029/JB089iB13p11527.
93. Baumgärtner J. *Anwendung des Hydraulic-Fracturing-Verfahrens für Spannungsmessungen im geklüfteten Gebirge, dargestellt anhand von Meßergebnissen aus Tiefbohrungen in der Bundesrepublik Deutschland, Frankreich und Zypern*; 1987. Berichte des Instituts für Geophysik der Ruhr-Universität Bochum A/21.
94. Baumgärtner J, Rummel F. Experience with “fracture pressurization tests” as a stress measuring technique in a jointed rock mass. *International Journal of Rock Mechanics and Mining Sciences & Geomechanics Abstracts*. 1989;26(6):661-671. doi:10.1016/0148-9062(89)91446-0.
95. Savage WZ, Swolfs HS, Powers PS. Gravitational stresses in long symmetric ridges and valleys. *International Journal of Rock Mechanics and Mining Sciences & Geomechanics Abstracts*. 1985;22(5):291-302. doi:10.1016/0148-9062(85)92061-3.
96. MeSy. *CBM - Project Sigillaria License Area. Cased-Hole Permeability Measurements in Borehole Natrap-1. Final Report: Report No. 23.96*. [internal report in German]; 1996. https://fordatis.fraunhofer.de/bitstream/fordatis/290/1/Cased_hole_permeability_and_stress_measurements_in_borehole_Natrap1_final_report_23_96.pdf.
97. Rummel F. Crustal Stress Derived from Fluid Injection Tests in Boreholes. [6]. In: Sharma VM, Saxena KR, eds. *In-Situ Characterization of Rock*. A.A. Balkema Publishers; 2002:205-244.
98. Kruszewski M, Montegrossi G, Backers T, Saenger EH. In Situ Stress State of the Ruhr Region (Germany) and Its Implications for Permeability Anisotropy. *Rock Mech Rock Eng*. 2021;54(12):6649-6663. doi:10.1007/s00603-021-02636-3.
99. Morris A, Ferrill DA, Brent Henderson D. Slip-tendency analysis and fault reactivation. *Geol*. 1996;24(3):275. doi:10.1130/0091-7613(1996)024<0275:STAAFR>2.3.CO;2.
100. Niederhuber T, Müller B, Müller L, et al. *Slip tendency of faults and pore pressure evolution in the “Wasserprovinz Haus Aden” – Ruhr area*. Deutsche Geologische Gesellschaft - Geologische Vereinigung e.V. (DGGV); 2021.
101. Bischoff M, Cete A, Fritschen R, Meier T. Coal Mining Induced Seismicity in the Ruhr Area, Germany. *Pure appl geophys*. 2010;167(1-2):63-75. doi:10.1007/s00024-009-0001-8.

102. Wehling-Benatelli S, Becker D, Bischoff M, Friederich W, Meier T. Indications for different types of brittle failure due to active coal mining using waveform similarities of induced seismic events. 2013;4(2):405-422. https://se.copernicus.org/articles/4/405/2013/.
103. Engelder T, Sbar ML. Near-surface in situ stress: Introduction. *J Geophys Res*. 1984;89(B11):9321. doi:10.1029/JB089iB11p09321.

Declaration of interests

☒The authors declare that they have no known competing financial interests or personal relationships that could have appeared to influence the work reported in this paper.

☐The authors declare the following financial interests/personal relationships which may be considered as potential competing interests:

Highlights

- Hydraulic fracturing results in mines are affected by stress concentrations.
- Estimation of regional stress requires knowledge of pore pressure.
- Ruhr Area is characterized by normal faulting tectonics.